



# Assessing the impacts of the urban heat island effect on streamflow patterns in Ottawa, Canada



Jan Adamowski<sup>a,\*</sup>, Andreas Prokoph<sup>b</sup>

<sup>a</sup> Department of Bioresource Engineering, McGill University, 21 111 Lakeshore Road, Ste. Anne de Bellevue, QC, H9X 3V9 Canada

<sup>b</sup> SPEEDSTAT, 19 Langstrom Crescent, Ottawa, ON, K1G 5J5 Canada

## ARTICLE INFO

### Article history:

Received 10 March 2013  
 Received in revised form 13 May 2013  
 Accepted 15 May 2013  
 Available online 23 May 2013  
 This manuscript was handled by Andras Bardossy, Editor-in-Chief, with the assistance of Ashish Sharma, Associate Editor

### Keywords:

Wavelet transform  
 Urban heat island effect  
 Climate change  
 Urban water  
 Streamflow  
 Canada

## SUMMARY

Due to a variety of commercial and residential activities, large metropolitan areas in mid-to-high latitudinal ranges are experiencing rising air temperatures compared to their surrounding rural areas. This study investigated how this urban heat island effect (UHIE) may influence the streamflow of rivers crossing large urban areas on annual and multi-decadal time-scales. In order to detect, link, and quantify differences in meteorological and streamflow patterns between rural and large urban areas, this study developed a methodology based on the continuous wavelet transform (CWT), cross-wavelet transform (XWT), linear regression, as well as the Mann–Kendall (MK) test. A case study was carried out for the city of Ottawa, Canada as the metropolitan centre, along with three surrounding rural locations (Angers, Arn-prior, Russell), with pristine rivers crossing these locations. From roughly 1970 to 2000, air temperature in Ottawa increased at a rate exceeding 0.035 °C/year, while parallel changes in rural areas were relatively stable, and varied by less than 0.025 °C/year. The urban warming that occurred during these decades was accompanied by a significant drop in the amplitude of annual temperatures (i.e. warmer winters). Precipitation in both urban and rural areas showed no significant trends, although the variability in the precipitation amount decreased in both settings. Concurrently, streamflow showed decreasing trends in both urban and rural areas. Annual amplitudes in urban streamflow (Rideau River through Ottawa, ON) correlated positively with annual air temperature amplitudes (i.e., less severe annual flooding with a decreasing winter/summer temperature contrast), whereas such a relationship was not apparent for the rural stations. Moreover, the timing of the annual daily minimum temperature cycle correlated significantly with the streamflow pattern in the urban area, i.e., early annual warming corresponded to earlier annual streamflow maxima. The precipitation pattern (i.e. distribution of rain and snowfall over time) significantly influenced the annual and long term streamflow pattern, but this influence differed little between urban and rural areas. It was also determined that the warming from the urban heat island effect, especially during winter months, was found to perhaps reduce the severity of the annual spring flood event in mid-to-high latitudinal continental settings.

© 2013 Elsevier B.V. All rights reserved.

## 1. Introduction

The expansion of urban centers has created, over the years, a pronounced warming in urban areas relative to their rural surroundings (Oke, 1973; Karaca et al., 1995; Arnfield, 2003). There are several mechanisms caused by urbanization that can influence streamflow. This includes human induced changes such as changes through construction, river flow regulation to water outfall and heated water disposal, as well as natural factors that are influenced by urbanization. These mechanisms include altered natural causes such ambient air temperature increases and altered precipitation

patterns in urban centers. These altered natural mechanisms can lead to earlier snowmelt in the year, as well as changes in precipitation related runoff resulting in changes in temporal streamflow patterns compared to the rural surroundings. These differences in air temperatures in city centers, first observed by Howard (1833) as early as the 19th century, were eventually coined under the term “Urban Heat Island” (UHI) by Manley (1958), when he was investigating changes in snowfall patterns between rural and urban areas. Over the years, research has shown that as population increased and cities grew, so did the intensity of their UHIE (Oke, 1973; Li et al., 2004). It has also been observed that the UHIE provides additional warming to both an urban center and its immediate surrounding areas, and that this warming is more pronounced during the winter months when commercial and residential heating are at their highest (Karl et al., 1988).

\* Corresponding author. Tel.: +1 5143987786.

E-mail addresses: [jan.adamowski@mcgill.ca](mailto:jan.adamowski@mcgill.ca) (J. Adamowski), [aprokocn@aol.com](mailto:aprokocn@aol.com) (A. Prokoph).

UHIs have been studied in various parts of the world (Arnfield, 2003), with locations ranging as far as Alaska in northern latitudes (Hinkel et al., 2003) and in warmer and drier regions such as Spain and Turkey (e.g., Yague and Zurita, 1991; Karaca et al., 1995; Montávez et al., 2000; Yalcin and Yetemen, 2009). With regards to Canada, Oke has investigated temperature trends in urban centers in the St-Lawrence Lowlands as well as in the Pacific Northwest (Oke, 1973; Oke and Maxwell, 1975), with current research now focused in detecting correlations between meteorological conditions and the intensity of the UHI phenomenon in central Canadian cities such as Toronto and Regina (Stewart, 2000; Moshin and Gough, 2012).

While research on the UHIE has been previously geared towards identifying the effect of urban warming on ambient air temperatures, there has been in recent years some research that investigates the possible effect of urban heating on water resources. For example, Shepherd and Burian (2003) and Lin et al. (2011) have examined the impact of UHIs on rainfall anomalies in coastal areas. Their research showed that urban centers located near water masses are becoming warmer and drier because higher rates of evaporation in urbanized areas are blocking precipitation formation by inhibiting water vapor from being transported from the coast. Kinouchi et al. (2007) also investigated the effect of UHIs on water sources by looking at increases in stream temperatures related to heat inputs from urban wastewater. Their study revealed that there was a correlation between increases in urban stream temperatures and increases in urban wastewater temperatures, which they expect to increase even more in the future due to higher urbanization rates and a rise in energy demand and water consumption. More recently, Yalcin and Yetemen (2009) have brought forward the idea that UHIs can also have an impact on groundwater resources. From their analysis of temperature data in underground layers of streams and wells near Istanbul, they observed that the water temperatures in urban groundwater sources were on average 3.5 °C higher than the rural groundwater sources.

Whereas it can be seen from the above examples that research involving the UHIE on water resources is slowly gaining momentum, there is still a lack of studies that directly examine the effect of UHIs on urban streamflow patterns and variability, with past research having been predominately focused on rural streamflows (Lettenmaier et al., 1994; Krakauer and Fung, 2008). Zhang et al. (2001) determined that, in general, streamflow in Canadian rivers had decreased over the last 30–50 years, except for the months of March–April when spring streamflow had increased. Projected global climate warming over the coming century will clearly influence streamflow patterns in snowmelt-induced annual discharge cycles typical of mid-to-high-latitude continental climate settings, especially with regards to the patterns' magnitude and onset (Douglas et al., 2000). Many large, heavily populated urban centers such as Ottawa, Minneapolis, Chicago, Berlin, Kiev and Moscow are located in mid to high latitude continental settings. It thus becomes very important to characterize the effect of UHIE on the streams that are found within these particular urban centers.

Both wavelet analysis and the Mann–Kendall test have been used (although not together) to determine streamflow trends and other patterns, as well as to analyze climate records in Canada. The Mann–Kendall test (Yulianti and Burn, 1998) and wavelet analysis (e.g., Anctil and Coulibaly, 2004; Abdul Aziz and Burn, 2006; Burn et al., 2008; Adamowski et al., 2009) have been predominately used in determining long-term (multiannual) trends and relationships. These studies found a positive correlation between streamflows and patterns of both the El-Nino/Southern Oscillation (ENSO) and the North Atlantic Oscillation (NAO). They also revealed a shift in these streamflow patterns between 1950 and 1970. Nakken (1999) also used wavelet analysis to investigate the potential anthropogenic influences on streamflow, focusing

specifically on the rainfall-streamflow pattern, and finding a strong relationship between them.

The purpose of this study is twofold: (i) Develop a criterion to determine and quantify the influence of overlying long-term regional and global climate trends on river flow patterns. Waveband-specific trends and climate-streamflow relationships which have been found to occur can be best addressed by using wavelet and cross-wavelet transform-based amplitude and phase-lag extraction techniques and significance of trend evaluations using Mann–Kendall tests and assessments of the significance of linear correlations. The aim is to determine if streamflow is significantly influenced by UHIE and, if so, at which wavelengths (time-scale). (ii) Complete a case study for Ottawa, Canada focusing on multi-decadal vs. annual timescale impacts of meteorological variations on river flow patterns, based on continuous daily records from 1972 to 1998. Drawing on several rural and urban monthly climate records, Prokoph and Patterson (2004) used wavelet and trend analysis to determine the impact of the UHIE in the Ottawa area. Over the last fifty years, UHIE warming in Ottawa has occurred at a mean rate of 0.009 °C/yr, and has, in turn, strongly raised regional background warming to a rate of roughly 0.006 °C/yr. Particularly large increases in urban–rural temperature differences occurred during periods of accelerated population growth in Ottawa. Their results provide the basis for the climate record analysis undertaken in this study.

## 2. Methodological approach

The ability to access extensive streamflow and climate records (e.g. temperature, total precipitation) for Ottawa and its surrounding areas was an important aspect of this study. The records provided information on daily streamflow changes for rivers flowing from a rural area into a high heat-island-affected city centre. For this study, one pair of daily and monthly records from urban streamflow/meteorological stations, and, as a control set, a rural streamflow/meteorological pair of station records, were chosen for detailed comparison. Data from Environment Canada (weather.ec.gc.ca, and ec.gc.ca/rhc-wsc) was used as the primary source of data for these observations. In this case study, the streamflow discharge ( $F$ ), both at daily- and monthly-averaged sampling rates were used as hydrological dependent records, while different types of precipitation ( $P$ ) and air temperature records served as independent records. Other climate-related records such as evapotranspiration, snow-on ground/day, snowmelt/day or daily and monthly extreme values were not available at sufficient continuity to be used for this study. Monthly mean temperature ( $T$ ), daily maximum temperature ( $T_{\max}$ ) and daily minimum temperature ( $T_{\min}$ ) were used in this study. Monthly records are sufficient to analyse the general annual pattern, but important information is lost concerning diurnal fluctuations, represented by  $T_{\min}$  and  $T_{\max}$ , that are important in characterizing UHIE (e.g., Karl et al., 1988). Ten methodological steps were carried out in this study to determine the potential influence of the UHIE on long-term and annual streamflow patterns (Fig. 1):

- (i) Gathering pairs of nearby (<5 km apart) streamflow and climate records over the same time-interval, at the same sampling rate, and preferably with perfect completeness. These records were then grouped into potential UHIE influenced (urban) and non-influenced (rural) records.
- (ii) Calculating descriptive statistics for each record to provide an overview of distribution and extreme values. This process was aided by visual observation of the plotted records.
- (iii) Calculating and evaluating each record's sample distribution with regard to Gaussianity, a prerequisite for optimal signal detection and extraction using Fourier analysis and the

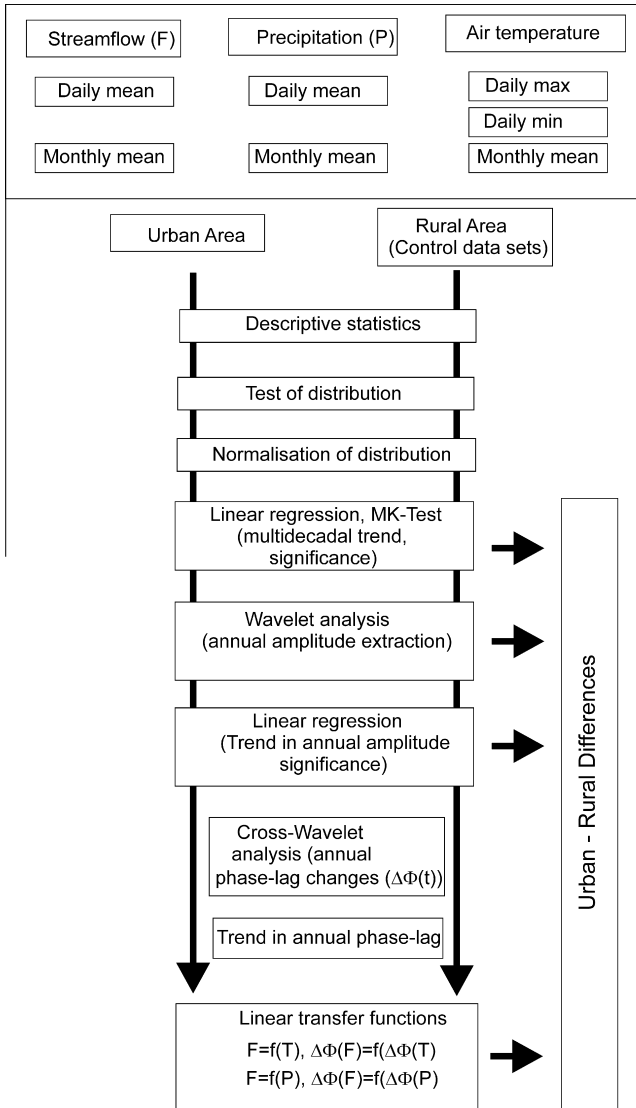


**Fig. 1.** Flow diagram for processing of both urban heat island affected “URBAN” and unaffected (“RURAL”) areas.

wavelet transform. In this study, the latter was done using the Morlet wavelet. It should be noted that the distribution may not be scale-invariant, *i.e.*, a record may be non-Gaussianly distributed on a short time-scale but Gaussianly distributed on a long time-scale. We tested Gaussianity using the histogram methods of Al-Smadi (2005).

- (iv) Transforming non-Gaussian distributed records into Gaussian distributed records using lognormal or other case-specific transformation techniques adequate for hydrological data (Granato, 2009).
- (v) Determining long-term, usually multi-decadal trends for less than 100-year record lengths using linear regression, then testing the significance of the linear trend, using the non-parametric Mann–Kendall Test (Kendall, 1975). Consequently, records should preferably have exactly the same observation/sampling period.
- (vi) Extracting annual signals, in particular amplitudes as a function of time, using CWT (Prokoph and Barthelmes, 1996). In contrast to spectral analysis, CWT allows for the extraction of not only single (averaged) signal amplitudes, or spectral power and phase per waveband, but also time-dependent records which allow for the tracing of the signal through different urbanization stages.

- (vii) Applying linear regression and the MK Test with related significance testing on annual amplitude records.
- (viii) Applying cross wavelet analysis (XWT) to hydrological and climate data to extract changes in the annual phase-offset between paired urban and rural records.
- (ix) Determining whether the annual urban–rural phase-relationship remained stable or not over time, and using linear regression to determine if a trend occurs in the annual phase-lag changes.
- (x) Determining: (a) The significance of long-term and annual-scale relationships between climate-streamflow, and (b) If significant, differences in trends between urban–rural records were assessed by cross-plots and Pearson correlation coefficients. The annual amplitude and phase-lag record were downsampled to one data point per year to ensure non-autocorrelated, independent samples for significance evaluation. Differences in trends determined whether the influence of the UHIE on streamflow had an impact on long-term streamflow trends, annual amplitude of streamflow, or timing (phase-offset) of annual streamflow cycle fluctuations.

### 3. Data analysis methods

#### 3.1. Continuous wavelet analysis

The Continuous Wavelet Transform (CWT) allows for the automatic localization of periodic signals, gradual shifts and abrupt interruptions, trends and onsets of trends in time series (Rioul and Vetterli, 1991). In contrast to Fourier analysis, CWT permits the transformation of observed time series into wavelet coefficients according to time and scale (or frequency) simultaneously. These coefficients can be used to detect and estimate trends or to reconstruct signals in streamflow and meteorological records that are of interest for this study. Wavelet analysis first emerged as a filtering and data compression method in the 1980s (e.g., Morlet et al., 1982a,b). Wavelet analysis transforms a time-series into a frequency domain, then simultaneously transforms the ‘depth’ or ‘time’ domain and the ‘scale’ or frequency domain by using various shapes and sizes of short filtering functions called ‘wavelets.’ The wavelet coefficients  $W$  of a time series  $x(s)$  are calculated by a simple convolution (Prokoph and Barthelmes, 1996):

$$W_{\psi}(a, b) = \left( \frac{1}{\sqrt{a}} \right) \int x(s) \psi \left( \frac{s-b}{a} \right) ds \quad (1)$$

where  $a$  is the scale factor that determines the characteristic frequency or wavelength,  $b$  represents the shift of the wavelet over  $x(s)$ , and  $\psi$  is the mother wavelet; the variable.

The bandwidth resolution for a wavelet transform varies with  $\Delta a = \frac{\sqrt{2}}{4\pi a^2}$ , and a location or time resolution  $\Delta b = \frac{a}{\sqrt{2}}$ . Note that due to Heisenberg’s uncertainty principle  $\Delta a \Delta b \geq 1/4\pi$ , and the resolution of  $\Delta b$  and  $\Delta a$  cannot be arbitrarily small (e.g., Prokoph and Barthelmes, 1996). Parameter  $l$  is used to modify wavelet transform bandwidth resolution either in favour of time or in favour of frequency. In this study, the CWT was used with the Morlet wavelet as the mother function (Morlet et al., 1982a,b). The shifted and scaled Morlet mother wavelet is defined as:

$$\psi_{l,a,b}(s) = \sqrt[3]{\pi} \sqrt{a} l e^{-\frac{l^2 \pi (s-b)^2}{a}} e^{-\frac{1}{2} \left( \frac{s-b}{a} \right)^2} \quad (2)$$

The Morlet wavelet is simply a sinusoid with wavelength/period  $a$  modulated by a Gaussian function (Torrence and Compo, 1998; Prokoph and Patterson, 2004; Adamowski, 2008). Edge effects of the wavelet coefficients occur at the beginning and end of the analysed time-series and increase with increasing wavelength (scale) and with the  $l$  parameter forming a ‘cone of influence of edge ef-

fects' (about 5% in this study) (Torrence and Compo, 1998). The wavelet coefficients  $W$  are represented in this study by the amplitude of Fourier frequencies by replacing  $\sqrt{a}$  with  $a$ . The parameter  $l = 6$  was chosen for all analyses, which gives sufficiently precise results in resolution of depth and frequency, respectively (Ware and Thomson, 2000; Adamowski, 2008). The wavelet analysis technique used in this article is explained in greater detail by Prokoph and Barthelmes (1996) and Adamowski et al. (2009).

In this study, wavelet coefficients were calibrated to reduce their exponential decay due to edge effects by dividing the wavelet coefficient of wavelength  $a$  extracted from Eq. (1) by a standing sine wave of amplitude 1 and wavelength of 365 days. The matrix of the wavelet coefficients  $W_l(a,b)$ , or the so called 'scalogram', was coded with shades of grey for superior graphical interpretation. The scale with the strongest wavelet coefficient in the 320–400 day waveband, and its associated wavelet coefficient and phase, were extracted for each time interval  $\Delta b$ .

The differences in CWT compared to spectral analysis for the purpose of this study (extractions of records of amplitudes of annual signals) are illustrated in Fig. 2. A set of three deterministic models with record lengths in model units (mu)  $t = 0 \dots 200$  were constructed:

**Model 1:**  $y(t) = 0.01t[1 + \cos(\frac{2\pi t}{12})]$  implements a stationary annual signal of gradually increasing amplitude with the addition of an underlying linear trend. This model can represent long-term gradually-increasing streamflow, as well as increased annual low-high streamflow amplitudes.

**Model 2:**  $y(t) = \exp(0.01t)[1 + \cos(\frac{2\pi t}{12})]$  has the same structure as model #1, but is exponentially enhanced.

**Model 3:**  $y(t) = 0.01t[1 + \cos(\frac{2\pi t}{12 - 0.01t^2})]$  represents a 'chirp' (Mann and Haykin, 1992) with a synchronous increase of amplitude and frequency due to a resonance effect, which can represent an earlier arrival of the annual snowmelt-induced flood paralleled by increasing flood amplitude.

In contrast to spectral analysis (Fig. 2B, D and F), CWT is able to trace and extract the temporal signal changes, in particular for Model 3 (Fig. 2E), where spectral analysis provides a low-spectral power distributed over a broad waveband (Fig. 2F). However, the period doubling of the annual signal in both spectral analysis and CWT with model 2 (Fig. 2C and D) illustrates the importance of transforming, in this case exponentially, a non-Gaussian distributed signal into a Gaussian-distributed record to avoid amplitude loss in the waveband of interest. Moreover, the autocorrelation of the original and the reconstructed signal is preserved (Fig. 3H). Thus, autocorrelation of amplitudes extracted from annual signals of climate or streamflow records will not be biased, except for some cases, as in model 2, and no bias will be introduced in evaluating the significance of trends.

### 3.2. Cross-wavelet analysis (XWT)

The cross-wavelet spectrum of two series  $x(t)$  and  $y(t)$  is defined by:

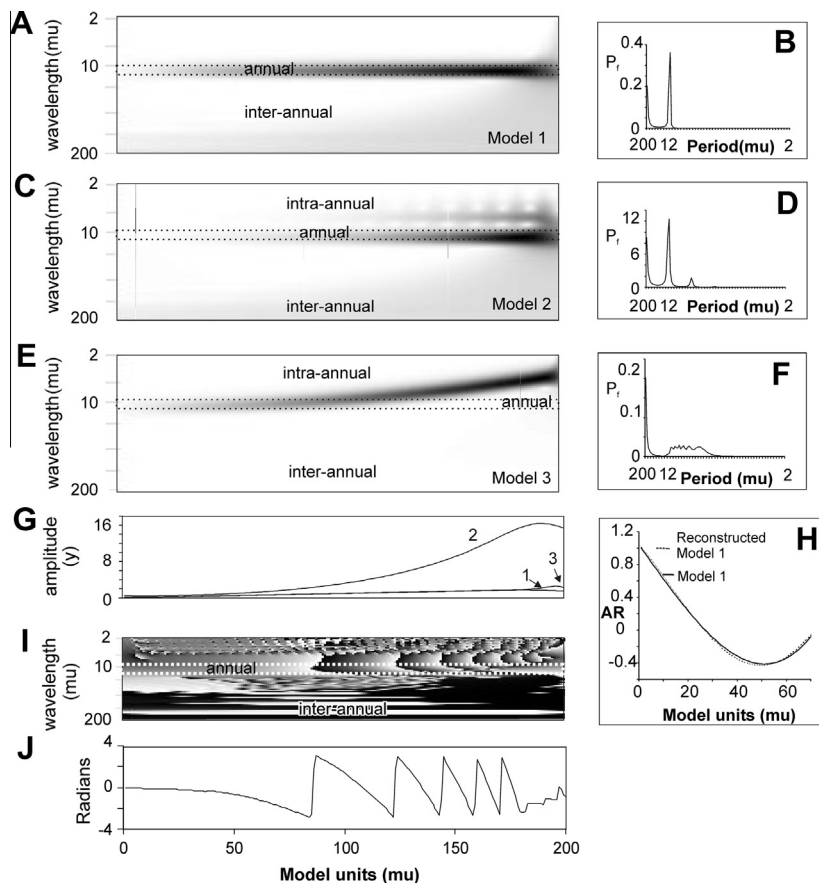


**Fig. 2.** Wavelet (CWT), cross wavelet (XWT) and spectral analysis (SA) to detect annual and long-term nature of UHIE for model units (mu)  $t = 0 \dots 200$ . (A) CWT and (B) SA of Model 1:  $y(t) = 0.01t + 0.01t \cos(2\pi t/12)$ . (C) CWT and (D) SA of Model 2:  $y(t) = \exp(0.01t + 0.01t \cos(2\pi t/12))$ . (E) CWT and (F) SA of a "chirp" Model 3:  $y(t) = 0.01t + 0.01t \cos(2\pi t/(12 - 0.01t^2))$ . (G) Extracted maximum annual amplitudes, corrected for edge effects. (H) Autocorrelations of amplitudes of Model 1 and reconstructed Model 1. (I) Phase spectrum of chirp (Model 3) versus  $y(t) = 0.01t \cos(2\pi t/12)$ . (J) Extracted phase lag of annual waveband (11–13 model units bandwidth) from (I). Wavelet scalogram using Morlet wavelet with window width of 6, striped line marks >10% edge effect influence (below line), black-dark grey: large signal, white-low/no signal with intra-annual band (5–320 days), annual band (320–400 days) and inter-annual band (400 days –  $2 \times$  total number of days).



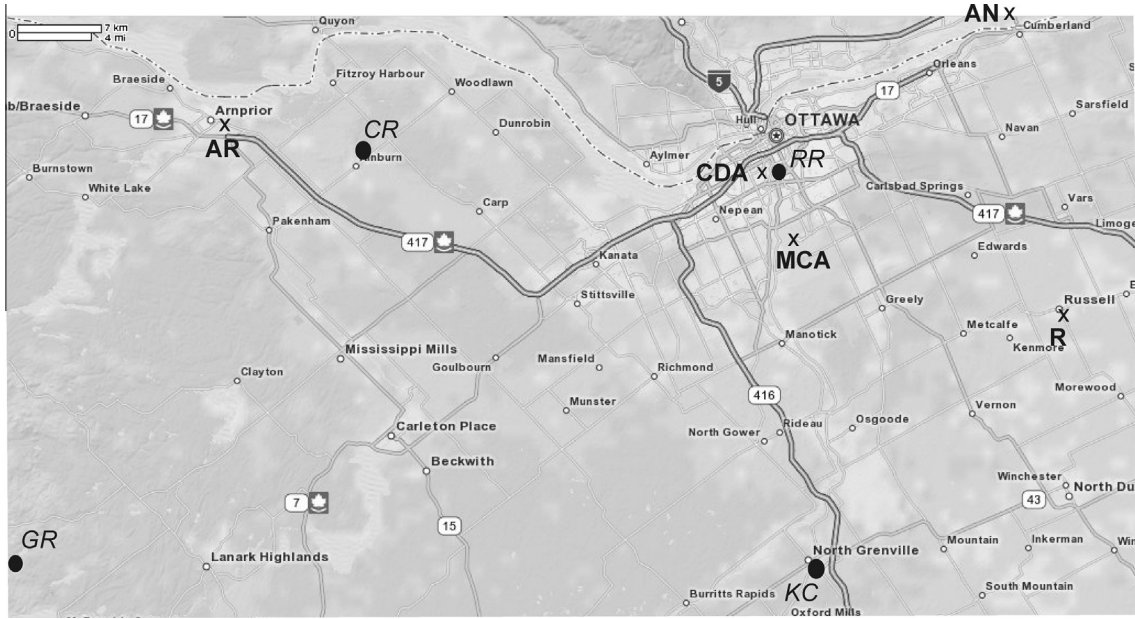


Fig. 3. Ottawa, Ontario map with meteorological stations (bold) and hydrological stations (italic): AR-Arnprior, CDA-Ottawa CDA, MCA-Ottawa MacDonal-Cartier Airport, AN-Angers, R-Russell, CR-Carp River at Kinburn, GR-Clyde River at Gordon Rapids, KC-Kemptville Creek at Kemptville, RR-Rideau River in Ottawa.

$$W_{xy}(a, b) = W_x(a, b)W_y^*(a, b) \quad (3)$$

where  $W_x(a, b)$  and  $W_y(a, b)$  are the CWT of  $x(t)$  and  $y(t)$ , respectively, and  $*$  denotes the complex conjugate (e.g., Jury et al., 2002). The phase difference is defined as:

$$\Delta\phi(b) = \tan^{-1} \frac{\int_{a1}^{a2} \text{Im}(W_{xy}(a, b)) da}{\int_{a1}^{a2} \text{Re}(W_{xy}(a, b)) da} \quad (4)$$

where  $b$  is the time lag  $b$  (Jury et al., 2002), and  $Im$  and  $Re$  represent the imaginary and real parts of the wavelet transform, respectively. The mother wavelet and parameters used in this study are the same as for the CWT description provided above. More details on the XWT technique that was used in this study can be found in Maraun and Kurths, (2004); Labat, (2008). They found that significance testing of the cross-wavelet amplitude, or the often used cross-wavelet coherency, is ambiguous. In this study, XWT was used to extract the phase lag between two records at a specific (here, annual) waveband  $\Delta\phi(b) = \Delta\phi(t)$ . The gradual changes in the phase shift can be properly traced and extracted as demonstrated by the XWT of model 3 compared to a cosine wave with a wavelength of 12 model units (Fig. 21 and J).

### 3.3. Mann–Kendall test

The Mann–Kendall test is based on the rank correlation methodology introduced by Kendall (1975) with associated statistical tests implemented by Gilbert (1987). The Mann–Kendall test can be applied when the data values  $x_i$  of a time series can be assumed to obey the model:

$$X_i = f(t_i) + \varepsilon_i \quad (5)$$

where  $f(t_i)$  is a continuous monotonic increasing or decreasing function of time, where  $\varepsilon_i$  (the residuals), are assumed to be from the same distribution and have a mean of zero (e.g., Salmi et al., 2002). The variance in the distribution is thus assumed to be constant in time. The null hypothesis of no trend existing,  $H_0$ , (i.e., the observations  $x_i$  are randomly ordered in time) was tested against the alternative hypothesis,  $H_a$ , assuming there to be an increasing or decreasing monotonic trend. The software MAKESENS

(Salmi et al., 2002), was used to calculate the Mann–Kendall test, which is based upon the normal approximation using  $Z$  statistics.

Let  $x_1, x_2, \dots, x_n$  represent  $n$  data points where  $x_j$  represents the data point at time  $j$ . Then the Mann–Kendall statistic ( $S$ ) is given by (Kendall, 1975):

$$S = \sum_{j=1}^{j=n} \sum_{k=1}^{k=n} \text{sign}(x_j - x_k) \quad (6)$$

where  $\text{sign}(x_j - x_k)$  equals 1 if  $x_j - x_k > 0$ , equals 0 if  $x_j - x_k = 0$ , and equals  $-1$  if  $x_j - x_k < 0$

A very high positive value of  $S$  is an indicator of an increasing trend, while a very low negative value indicates a decreasing trend. However, it is necessary to compute the probability associated with  $S$  and the sample size,  $n$ , to statistically quantify the significance of the trend.

The variance (VAR) of  $S$  is computed by the following equation:

$$\text{VAR}(S) = 1/18(n(n-1)(2n+5) - \sum t_p(t_p-1)(2t_p+5)) \quad (7)$$

where  $n$  is the number of data points, and  $t_p$  is the number of data points in the  $p$ th group. A normalized test statistic  $Z$  is then calculated as follows:

$$Z = \frac{S-1}{\sqrt{\text{VAR}(S)}} \text{ if } S > 0 \quad (8)$$

$$Z = 0 \text{ if } S = 0 \quad (9)$$

$$Z = \frac{S+1}{\sqrt{\text{VAR}(S)}} \text{ if } S < 0 \quad (10)$$

The presence of a statistically significant trend is evaluated using the  $Z$  value. A positive value of  $Z$  indicates an upward trend, and a negative value a downward trend. The statistic  $Z$  has a normal distribution. To test for either an upward or downward monotone trend at a level of significance  $\alpha$ ,  $H_0$  is rejected if the absolute value of  $Z$  exceeds  $Z_{1-0.5\alpha}$ , which is provided by the standard normal cumulative distribution (e.g., Davis, 1986). The tested significance levels implemented in MAKESENS are  $\alpha = 0.001, 0.01, 0.05$  or  $0.1$ .

## 4. Data

### 4.1. Streamflow records

Located just south of Ottawa's centre, the Rideau River station was the primary source of streamflow data, whereas the other (non-urban) hydrological stations were located in streams in rural areas (Fig. 1). The Rideau River Authority provided digital records of two daily and four mean-monthly streamflow records; the Water Service of Canada website ([wsc.ec.gc.ca](http://wsc.ec.gc.ca)) was also used as a source of similar records. Complete records ranging from 1972–2005 were available for all stations, and some extended as far back as the 1930s (Table 1). The only streamflow records which were considered were those which showed stable land-use or pristine conditions, less than 5% missing data, and at least 20 years of properly monitored measurements, taken over the same time-interval as nearby meteorological stations. Furthermore, the records that were used are approved by the Water Service of Canada and/or the Rideau River Authority.

### 4.2. Climate records

Data was collected and accessed from various meteorological stations and weather and government sources. The three rural stations under study were located in Arnprior, Russell, and Angers, Ontario, and represented areas with rural climates. The stations were located in small towns with populations under 25,000 (Fig. 3). The urban area of Ottawa centre was represented by the Canadian Department of Agriculture (CDA) station approximately 2 km south of downtown Ottawa, and about 4 km east from the Rideau River hydrological station. The Ottawa MCA (MacDonald–Cartier Airport) station is situated in a suburban area gradually shifting from a rural to an urban setting. The meteorological data analyzed during the study focused predominately on air temperatures and precipitation levels and were provided by Environment Canada ([weather.ec.gc.ca](http://weather.ec.gc.ca)). These were daily and monthly total precipitation, monthly mean temperature, and daily minimum and maximum temperatures (Table 1, Fig. 4). Based on continuous 24 h recordings, all climate records were approved for public and academic release by Environment Canada (2009) and as such were corrected and calibrated. Estimates, below detection limit mea-

surements or missing data were recorded. Only records that were more than 95% complete (i.e., that were not estimates or missing entries) were used. Priority was given to the urban climate-streamflow pairs of Ottawa CDA–Rideau River records and the rural Arnprior–Carp River pairs based on population difference, vicinity of the climate-streamflow pair and almost equivalent recording periods.

## 5. Results

### 5.1. Descriptive statistics and sample distribution of climate and streamflow records

During the case study, differences in meteorological and streamflow patterns within Ottawa (and the three surrounding rural areas of Arnprior, Russell, and Angers) were identified and quantified. The data analysis focused on pairs of streamflow-climate records that were obtained less than 10 km apart (see Fig. 3). The urban pair was the Rideau River at Ottawa, with Ottawa CDA, and the rural pair was the Carp River at Kinburn Side Road Bridge, and Arnprior. The climate records in all locations were nearly complete from 1972 to 1999, with a total of 10 days missing in 1982 and 1985 from the Arnprior records. All streamflow records show short and high annual discharge peaks due to snow melt with a long low discharge interval in between (Fig. 4A and B). The total amount of discharge varied depending on the magnitude of streamflow, with the Rideau River discharge roughly 10 times that of the rural streamflows (Table 1). The sample distribution of all the records was very similar, as indicated by their kurtosis and skewness (Table 1). The magnitudes of monthly mean temperature fluctuations were similar between all records, but these differed significantly in terms of precipitation records (see Fig. 4C and D). Moreover, histograms indicate that the temperatures were scale invariant and normally distributed, with a slight bi-modal pattern (Fig. 5A and B). The distribution was non-Gaussian for daily precipitation records, but Gaussian for monthly records. Thus, for the analysis of annual amplitudes in this study, a Gaussian distribution can be assumed. In contrast, streamflow data were not normally distributed on either daily or monthly scales (Fig. 5E and G), confirming the non-Gaussian (e.g., log-normal) distribution in streamflow time-series found in other studies (e.g., Schaeffli and Zehe,

**Table 1**  
Hydrological and meteorological stations and descriptive statistics.

Station name	Station ID	Type	Unit	Data Range	Mean	Median	Standard deviation	Kurtosis	Skewness	Range	total data range
Rideau River at Ottawa, daily	WSC02LA004	F	m <sup>3</sup> /s	1/1/72–14/7/2005	44.25	23.70	59.40	16.15	3.44	581.52	10/12/69–31/10/09
Kemptville Creek, daily	WSC02LA006	F	m <sup>3</sup> /s	1/1/72–14/7/2005	2.89	1.89	6.36	17.51	3.66	80.09	11/12/69–28/10/09
Carp River near Kinburn, daily	WSC02KF011	F	m <sup>3</sup> /s	1/1/72–14/7/2005	5.00	0.84	8.51	36.78	5.25	85.00	4/9/71–14/7/05
Clyde River, daily	WSC02KF013	F	m <sup>3</sup> /s	1/1/72–14/7/2005	3.22	1.72	4.98	29.99	4.23	87.99	9/9/71–31/12/07
Ottawa, CDA, monthly	6105976	T	°C	1/1/72–1/12/05	6.30	7.10	11.18	−1.29	−0.21	40.30	1/1/1889–1/12/06
Ottawa, Airport, monthly	6106000	T	°C	1/1/72–1/12/05	6.18	6.95	11.14	−1.27	−0.20	40.70	1/1/1938–1/12/06
Angers, QC, monthly	7030170	T	°C	1/1/72–1/12/05	4.92	5.70	11.20	−1.26	−0.23	41.10	1/1/1962–1/9/2009
Arnprior, monthly	6100345	T	°C	1/1/72–1/12/05	5.70	6.80	11.41	−1.27	−0.23	42.10	1/1/1959–9/9/1999
Russell, monthly	6107247	T	°C	1/1/72–1/12/05	6.32	7.20	10.98	−1.20	−0.25	40.30	1/1/1954–1/12/2006
Ottawa, CDA, monthly	6105976	P	mm	1/1/72–1/12/05	76.16	73.10	34.55	0.29	0.64	193.60	1/1/1889–1/12/06
Ottawa, Airport, monthly	6106000	P	mm	1/1/72–1/12/05	78.18	73.20	34.35	0.65	0.64	223.20	1/1/1938–1/12/06
Angers, QC, monthly	7030170	P	mm	1/1/72–1/12/05	82.11	76.00	39.17	0.58	0.74	209.30	1/1/1962–1/9/2009
Arnprior, monthly	6100345	P	mm	1/1/72–1/12/05	66.87	65.50	32.12	−0.19	0.50	174.00	1/1/1959–9/9/1999
Russell, monthly	6107247	P	mm	1/1/72–1/12/05	80.12	75.80	35.71	0.50	0.74	189.40	1/1/1954–1/12/2006
Ottawa, CDA, daily	6105976	P	mm	1/10/1972–9/9/1999	2.50	0.00	5.80	33.16	4.49	108.60	1/1/1889–1/12/06
Arnprior, daily	6100345	P	mm	1/10/1972–9/9/1999	2.20	0.00	5.36	26.16	4.21	76.00	1/1/1959–9/9/1999
Ottawa, CDA, daily	6105976	T <sub>max</sub>	°C	1/10/1972–9/9/1999	11.13	11.90	12.70	−0.90	−0.27	65.30	1/1/1889–1/12/06
Arnprior, daily	6100345	T <sub>max</sub>	°C	1/10/1972–9/9/1999	10.81	12.00	13.10	−0.90	−0.28	67.00	1/1/1959–9/9/1999
Ottawa, CDA, daily	6105976	T <sub>min</sub>	°C	1/10/1972–9/9/1999	1.65	2.60	11.82	−0.57	−0.47	59.80	1/1/1889–1/12/06
Arnprior, daily	6100345	T <sub>min</sub>	°C	1/10/1972–9/9/1999	0.80	2.00	12.21	−0.40	−0.54	63.00	1/1/1959–9/9/1999

T, air temperature; P, total precipitation; F, streamflow.

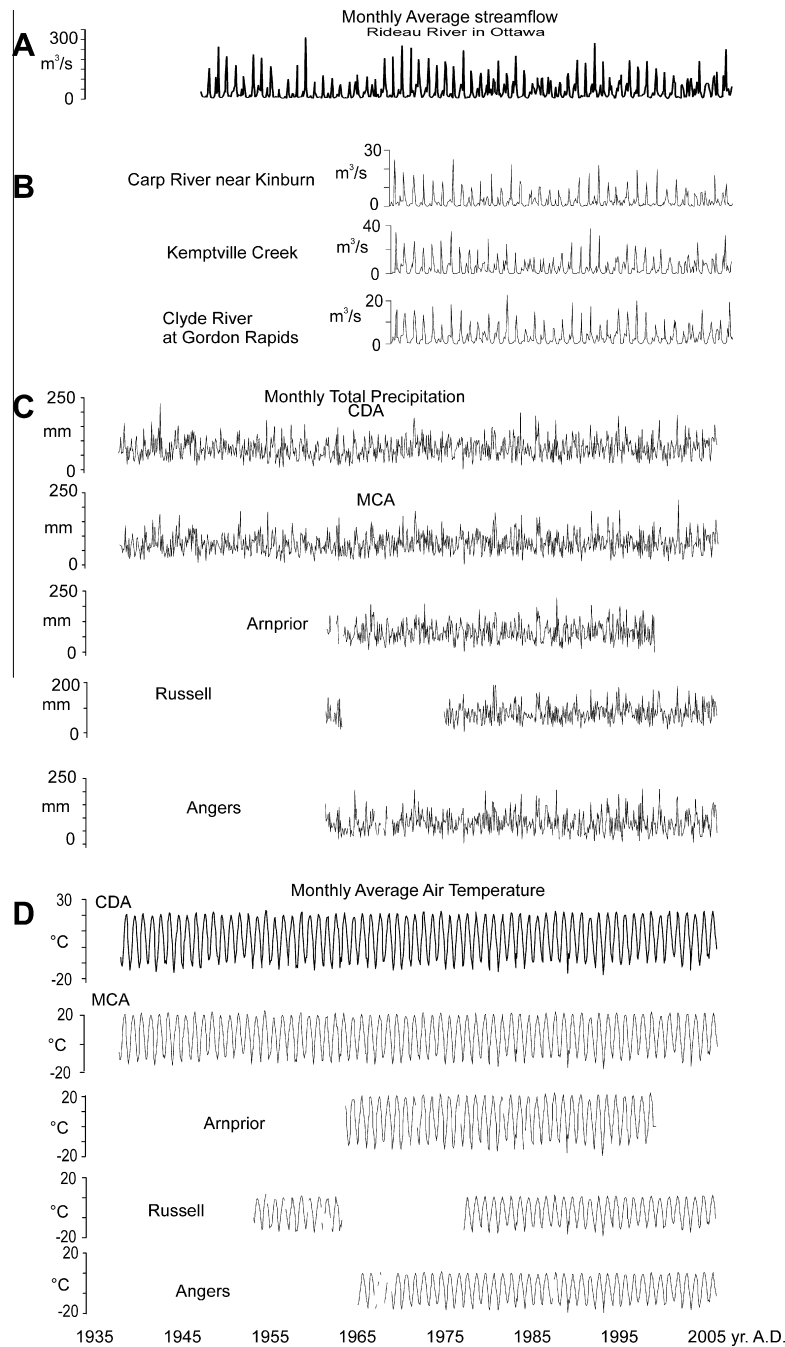


Fig. 4. Meteorological and hydrological monthly mean records from Eastern Canada.

2009). Thus, a log-normal transformation was required to provide a Gaussian distribution suitable for use in Morlet-wavelet-based CWT and XWT.

### 5.2. Long-term trends and pattern in climate and streamflow records

For the MK test and linear regression, climate records were downsampled into annual records for the years 1972–1999 for comparison with the streamflow records (Table 2). Neither of the annual mean records shows any significant trends with precipitation. Annual precipitation differences between both rural and both urban locations showed no significant trends (Table 2).

The relative difference between urban vs. rural warming was manifested by the difference between long-term trends in the ur-

ban Ottawa CDA, the semi-urban MCA records and the average of the three rural stations (Arnprior, Russell, and Angers) from 1979 to 1999. In support of the UHIE, the MK test and linear regression methods (Table 2) showed that the air temperature in the Ottawa city centre (Ottawa CDA station) warmed significantly ( $P \leq 0.01$ ) over this period, while at Ottawa’s periphery (Ottawa MCA) this trend was less significant ( $P \leq 0.05$ ), and not significant ( $P > 0.05$ ) in the surrounding rural areas. The air temperature at the Russell station showed a weakly significant warming trend between 1979 and 2005 ( $P \leq 0.10$ ) when the population grew by 5–14% per year, compared to a normal growth of less than 3% per year. This indicates an urban heat island effect of  $0.022 \text{ }^\circ\text{C/year}$  for Ottawa versus the surrounding rural areas (Table 2). The temperature trend difference between Ottawa CDA and the semi-urban MCA

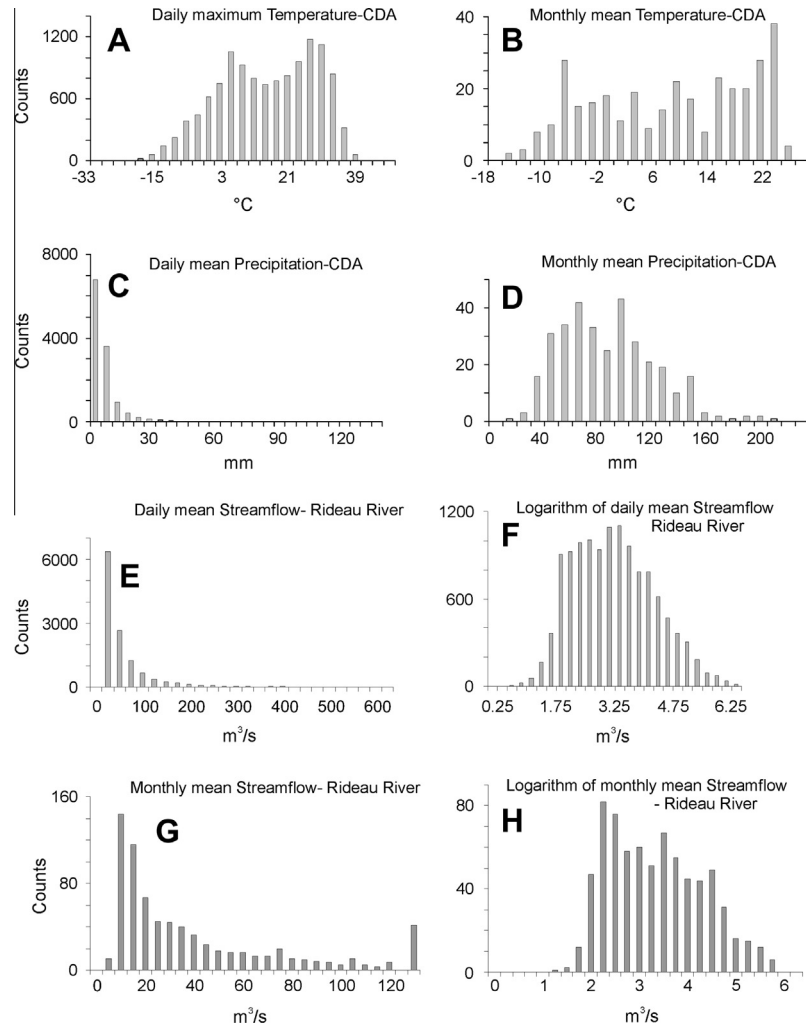


Fig. 5. Histograms of raw and logarithmic transformed meteorological and hydrological daily and monthly mean records.

**Table 2**  
Linear regression and Mann–Kendall tests of long-term changes: trends and significance.

Time series	Data type	First year	Last year	<i>n</i>	Mann–Kendall trend		Regression $y = at + b$	
					Test Z	Signific.	Trend( <i>a</i> )	<i>r</i>
Rideau River	<i>F</i>	1972	2006	35	−0.37		−0.097	0.12
Carp River	<i>F</i>	1972	2006	35	−1.05		−0.01	0.22
Kemptville Creek	<i>F</i>	1972	2006	35	−0.97		−0.019	0.20
Clyde River	<i>F</i>	1972	2006	35	−0.48		−0.005	0.09
Ottawa CDA	<i>T</i>	1972	2005	34	2.58	0.010	0.042	0.50*
Ottawa MCA	<i>T</i>	1972	2005	34	2.25	0.050	0.033	0.41*
Arnprior	<i>T</i>	1972	1998	27	1.04		−0.027	0.18
Russell	<i>T</i>	1979	2005	27	1.71	0.100	0.034	0.37
Angers	<i>T</i>	1972	2005	34	0.27		0.004	0.05
Ottawa CDA	<i>P</i>	1972	2005	34	−0.47		−0.102	0.12
Arnprior	<i>P</i>	1972	1998	27	0.71		0.124	0.17

*T*, annual mean air temperature; *P*, total daily precipitation, annual average; *F*, annual average streamflow; *n*, record length (in years); *r*–Pearson correlation coefficient.  
\* Level of significance >0.05.

station is minor (Table 2), likely due to increased construction and expansion activities around the airport between 1980 and 2000. The trend of annual streamflow records in both rural and urban hydrological stations was found to be weakly decreasing, but not significant ( $P > 0.05$ ) using either MK tests or linear regression analysis (Table 2).

Cross-plots and the  $R^2$  values of linear regressions of climate vs. streamflow (Fig. 6) indicate a significant dependency of streamflow

records on precipitation, but not on temperature. This correlation was more significant in the urban data than in the rural data (Fig. 6C and D). Thus, relative wet periods over several years led to long-term increases in the streamflow over the same period, particularly for the Rideau River. The Rideau River transports more water and has a larger drainage area than the smaller Carp River and may thus be more responsive to larger amounts of precipitation.



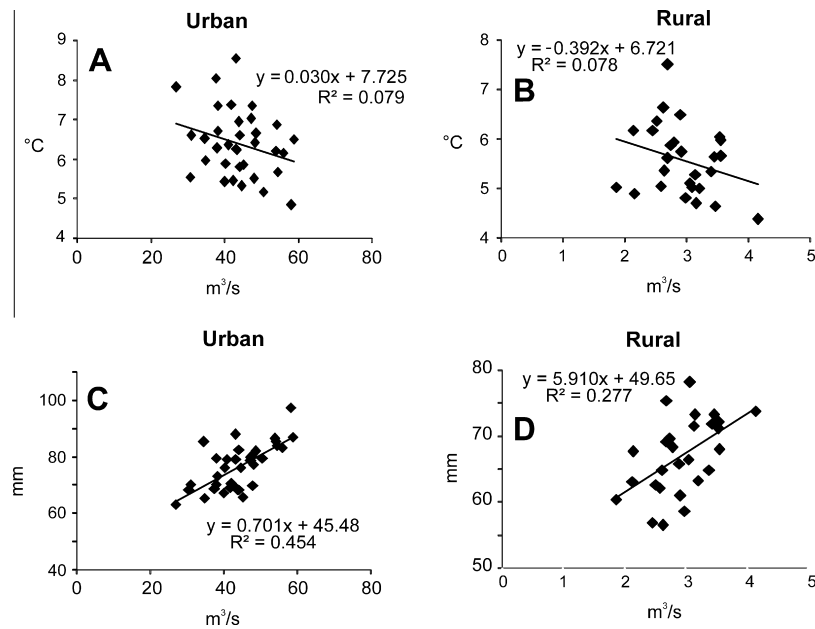


Fig. 6. Linear regression between mean annual meteorological and hydrological records from urban and rural areas with coefficient of determination ( $R^2$ ).

The rural area around the Carp River may be capable of releasing precipitation water through groundwater runoff more effectively. Alternatively, the weaker streamflow of the Carp River allows for a larger proportion of precipitation water to be removed from the streamflow by evaporation over the long term. However, this study indicates that the influence of precipitation on streamflow is the same in urban as in rural settings.

### 5.3. Impact of urban heat island effect on annual streamflow patterns

The CWT extracted the strongest signal for an annual amplitude in the 320–400 day waveband for all records from the urban Rideau River–Ottawa CDA and rural Carp River–Arnprior streamflow/weather station pairs (Fig. 7). Annual amplitude fluctuations were greater in the Rideau River with fluctuations of  $\approx 20 \text{ m}^3/\text{s}$  in years with a smaller difference between the annual snowmelt-induced discharge peak and base flow, and of  $\approx 50 \text{ m}^3/\text{s}$  in years when this difference was greater (Fig. 7A). The rural Carp River showed stronger relative fluctuations, as evidenced by the logarithmic-normalized record (Fig. 7B). Nevertheless, the temporal pattern was similar (Fig. 7A and B) with general negative trends. However, based on the MK test and Pearson correlation of both logarithmic normalized and non-normalized records, the annual amplitude trend was only significant in the rural Carp River (Table 3). This indicates that the contrast between high snowmelt-induced discharge and low baseflow significantly decreased over the study period, by either an increase in background flow or a decline in maximum flow.

The annual amplitudes of the climate records showed similar patterns between rural and urban records, with obvious negative trends in  $T_{\min}$  and  $T_{\max}$  (Fig. 7C–E). The annual amplitude of variability in total precipitation from 1973 to 1999 showed similar fluctuations, but no significant trends in either rural or urban areas (Fig. 7C). Both locations had simultaneous years of relatively constant precipitation and years that were characterized by large precipitation amplitudes (i.e. swings between rainy and dry seasons).

The annual amplitudes of daily  $T_{\min}$  and  $T_{\max}$  showed a distinctly different pattern between rural and urban areas (Fig. 7D and E). However, the MK test and Pearson correlations indicated that only the negative trends in the urban setting are significant

(Table 3). Years with relatively high and low annual temperature swings were still well correlated, but Ottawa's urban station (Ottawa CDA) showed only a slight linear decreasing trend from 1973 to 1999, indicating that the summer-winter temperature contrast became weaker over the years. This pattern is typical for the urban heat island effect (e.g., Karl et al., 1988).

The annual amplitude fluctuations of streamflow and precipitation were significantly correlated in both rural and urban areas (Fig. 8A and D). Thus, higher amounts of snowfall/rain lead to higher amplitudes of the snowmelt induced annual discharge cycle. This also indicates that local precipitation measurements describe the overall precipitation pattern and its influence on the drainage system of the streamflow of interest well in the study region. Urban areas with more variable precipitation over short distances may require more than “pinpoint” measurements to illustrate urban or rural precipitation patterns. In contrast, only the urban annual  $T_{\min}$  and  $T_{\max}$  amplitudes were significantly correlated ( $r^2 > 0.34$  and  $0.55$ , respectively) with annual variability in streamflow (Fig. 8E and F).

The phase difference of the annual waveband signal between urban and rural records shows a shift of  $\approx -0.017$  radians, indicating that the annual streamflow cycle of the Carp River lags  $\approx 1$  day behind the Rideau River in Ottawa (Fig. 9). There is an abrupt drop to  $\approx -0.8$  radians ( $\approx 1.5$  months) in 1988/1989, with a recovery to  $\approx -0.2$  in 1990 (Fig. 9A). The phase difference in precipitation between both settings is even higher:  $\pm 1$  radians on average, equivalent to  $\pm 2.5$  months, indicating a strong local variability of the occurrence time of precipitation events (Fig. 9B). Neither phase differences in streamflow nor precipitation showed any significant trend (Table 3). In contrast, the phase difference of the annual cycle between urban and rural areas developed from  $\approx 0$  to  $\approx -0.03$  ( $\approx 2$  days) for daily  $T_{\min}$  (Fig. 9C) and to  $\approx -0.013$  ( $\approx 1$  day) for daily  $T_{\max}$  (Fig. 9D), both of which were statistically significant (3). Moreover, there was a significant positive correlation between phase differences in streamflow and  $T_{\min}$ , indicating that an earlier annual warming in the late 1980s in Ottawa vs. the rural areas, may have resulted in an early onset of snow-melt induced high discharge in the Rideau River compared to the Carp River, where the threshold for ice-breakup was not reached for several weeks after the Rideau River.

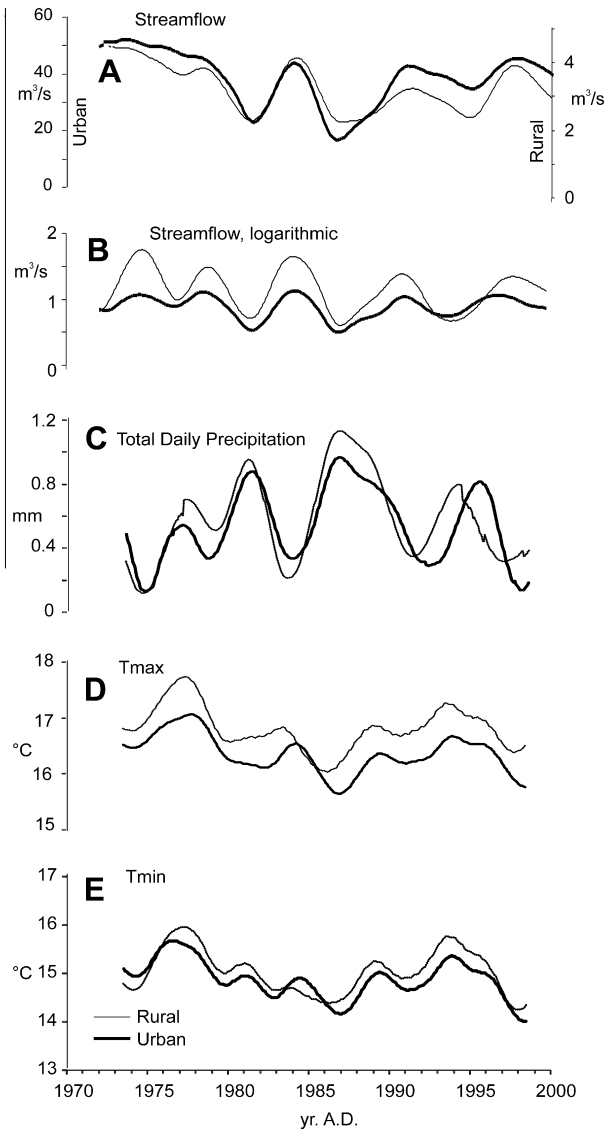


**Fig. 7.** Amplitudes of annual (320–400 days) waveband of urban (Ottawa CDA, Rideau River) and rural (Arnprior, Carp River) meteorological and streamflow records.

**Table 3**  
Mann–Kendall test of trends in annual amplitudes and phase of streamflow and climate records.

Time series	Data					MK trend		Regression $y = at + b$		Regression $\ln(y) = at + b$	
	Parameter	type	First year	Last year	$n$	Test Z	$\alpha$	Trend(a)	$r$	Trend(a)	$r$
RR	Amplitude	F	1974	1997	24	−1.36		−0.318	0.24	−0.002	0.09
CR	Amplitude	F	1974	1997	24	−1.71	0.1	−0.039	0.43**	−0.018	0.4**
CDA	Amplitude	P	1974	1997	24	0.72		0.006	0.17		
CDA- $T_{\min}$	Amplitude	T	1974	1997	24	−1.31		−0.018	0.39*		
CDA- $T_{\max}$	Amplitude	T	1974	1997	24	−1.41		−0.020	0.37*		
AR	Amplitude	P	1974	1997	24	−0.12		0.003	0.08		
AR- $T_{\min}$	Amplitude	T	1974	1997	24	−0.77		−0.010	0.16		
AR- $T_{\max}$	Amplitude	T	1974	1997	24	−0.62		−0.015	0.26		
RR-CR	Phase lag	F	1974	1997	24			−0.0390	0.17	0.0002	0.00
CDA-AR	Phase lag	P	1974	1997	24			−0.0185	0.31		
CDA-AR- $T_{\min}$	Phase lag	T	1974	1997	24			−0.0002	0.25		
CDA-AR- $T_{\max}$	Phase lag	T	1974	1997	24			−0.0002	0.45**		

$T$ , air temperature;  $P$ , total precipitation;  $F$ , streamflow;  $n$ , record length (in years); RR, Rideau River; CR, Carp River; CDA, Ottawa Canadian Department of Agriculture station; AR, Arnprior station;  $r$ -Pearson correlation coefficient.

\* Level of significance  $\alpha > 0.1$ .

\*\* Level of significance  $\alpha > 0.05$ .

## 6. Linkages in long-term and annual streamflows and climates

The long-term trends and correlations in the climate and hydrological records indicate a set of potential influences of UHIE on streamflow. However, the trends that were found are not related to the UHIE, but rather to regional or global variability. An influence of UHIE on long-term (multi-year) streamflow variability was not evident from our results. This is probably due to the suppression of the effects of local urban warming on precipitation by more influential, non-UHIE-mediated interannual changes, for example in precipitation, evaporation, and groundwater flow. For example, there was no significant relationship between long-term urban warming and mean streamflow discharge. The streamflow is, in the long-term, most strongly dependent on the precipitation pattern, which is not significantly impacted by the UHIE. In urban-heat-island-affected areas streamflow maxima peaked at lower values, but the large streamflows during the peak season were of longer duration than in rural areas. For example, large winter and summer flooding events occurred after high precipitation, whereas dry winters and wet summers were characterized by fewer and less extensive annual flooding events. The most significant detected impact of UHIE on streamflow occurred within the annual cycle, where the amplitude of temperature changes (both daily  $T_{\min}$  and  $T_{\max}$ ) were significantly correlated to streamflow amplitude changes, conferring the possibility of transfer functions.

The transfer function between temperature  $T$  ( $^{\circ}\text{C}$ ), and streamflow  $F$  ( $\text{m}^3/\text{s}$ ), was  $\Delta T/\text{year} \approx 0.025 \Delta F/\text{year}$ , or vice versa,  $\Delta F/\text{year} \approx 40 \Delta T/\text{year}$ . Thus, a reduction of  $\approx 1^{\circ}\text{C}$  in the annual winter cooling (or summer warming) may lead to a  $\approx 40 \text{ m}^3/\text{s}$  reduction in streamflow during the snowmelt induced annual discharge cycle. Over the last few decades the drop in the annual temperature amplitude at Ottawa CDA has been  $\approx 0.02^{\circ}\text{C}/\text{year}$  (Fig. 7D and E), which has resulted in a cumulative drop of  $\approx 0.8^{\circ}\text{C}$  over the last 40 years (Prokoph and Patterson, 2004). Based on the above relationship, this corresponds to a  $\approx 32 \text{ m}^3/\text{s}$  decrease in streamflow of the annual spring flood over the past four decades. This is a significant drop ( $>15\%$ ), considering that on average, the annual streamflow increases from an average baseflow of  $\approx 55 \text{ m}^3/\text{s}$  to over  $200 \text{ m}^3/\text{s}$  during the annual flood season; for the Rideau River, this season lasts one to two weeks. However, the absence of any significant correlation between air temperature and streamflow in the rural areas surrounding Ottawa underlines the impact and importance of the UHIE and the models used to detect it.

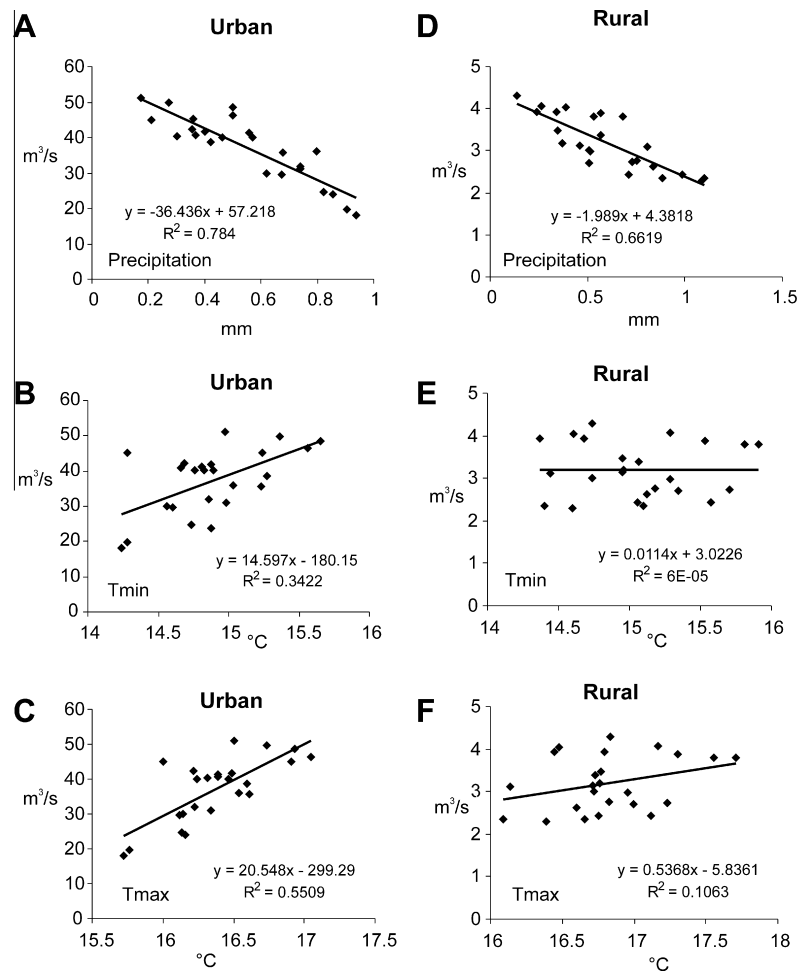


**Fig. 8.** Linear regression between annual amplitudes of meteorological and hydrological data from urban and rural areas with coefficient of determination ( $R^2$ ).

It was also found that a 1-day difference exists between urban and rural areas in the time lags between the onsets of the annual temperature cycle and streamflow cycle (Fig. 9). It is possible that this time-lag difference is caused by only a few extraordinary events during the late 1980s; more tests on longer datasets are required for stronger verification.

Previous studies have used combinations of wavelet analysis, regression analysis, or the Mann–Kendall test to explore waveband specific signals (e.g., Burn et al., 2008; Coulibaly, 2006). However, most of the previous studies focused on the relationship that exists between streamflow and long-term patterns, such as those seen with the North Atlantic Oscillation, or the sunspot and El Nino cycles (e.g., Anctil and Coulibaly, 2004; Adamowski et al., 2009). As well, no studies to date have used both wavelet analysis and the Mann–Kendall test together to explore the influence of climate on streamflow. This study determined, for the first time, in a quantitative manner, the impact of the urban heat island effect (i.e., urban warming) on the streamflow of rivers that flow through the center of their associated city. This study by no means exhausted all possible UHIE influences on river discharge. Including more climate related parameters and more study sites would provide a wider understanding. Moreover, higher-resolution records (e.g., hourly) may also detect diurnal dependency that could be useful for decision-makers involved with lock openings, waste overflow management and other issues. The methods used in this study (MK test, CWT and XWT) permit waveband-specific extraction and analysis of time-scale dependent changes that can provide

information beyond purely time-domain-averaged analyses such as those which use spectral techniques, or frequency-domain averaging analysis (e.g., smoothing and linear analysis). The use of time-independent correlation coefficients after the extraction stage already gives a good understanding of the UHIE, in particular for relatively short datasets such as the ones used in this study. For longer records the determination of time-dependent significance and coherency levels would be useful in tracing the development of an UHIE over time (e.g., a village growing into a large industrial city).

## 7. Conclusions

In this study, long-term (i.e. multi-annual) flow patterns were not significantly influenced by urban warming. However, annual flow patterns were significantly affected in the urban (vs. rural) area. The annual amplitude in the urban Rideau River streamflow in Ottawa correlated positively with the annual air temperature amplitude (i.e. less severe annual flooding with a decreasing winter/summer temperature contrast), whereas such a relationship did not occur at the rural stations. In the examples explored in this study, the annual flow pattern was strongly characterized by the magnitude and exact timing of the snowmelt-related high streamflow. Such snowmelt-induced annual discharge cycles are typical for most mid- to high-latitude and alpine streams in the northern hemisphere, which frequently pass through urban centers.

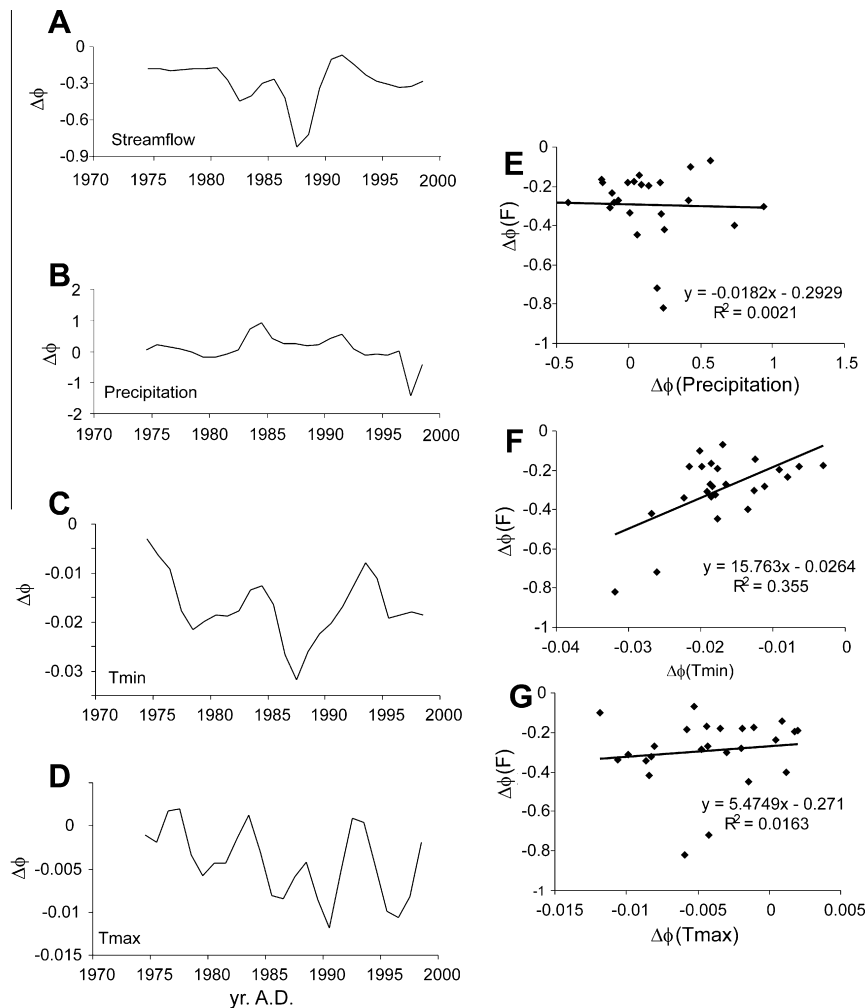


**Fig. 9.** Urban–Rural phase-lag differences in the annual waveband: (A–D) Records of phase-lag differences in the annual waveband of meteorological and hydrological data, note: 0.5 radians are equivalent to 1 month, and 0.017 radians are equivalent to 1 day. (E–G) Linear regression between phase-lag changes between urban and rural records of streamflow versus meteorological records, including coefficient of determination ( $R^2$ ).

This study also found that the precipitation pattern was not affected by urban heat island warming. The warming from the UHIE, especially during winter months, may reduce the severity of the annual spring flood event in mid-to-high latitudinal continental settings. Further studies could focus on the development of transfer functions between monthly or higher resolution climate records and corresponding streamflow measurements, as well as include other records that may be of importance to city planners and policy-makers in quantifying and projecting streamflow patterns (e.g., daily or monthly minimum or monthly flow) in a warming environment. For example, paired meteorological–streamflow measurements could be assigned for upstream and downstream regions of the urban center to evaluate the persistence and resilience of streamflow to the UHIE. The methodology presented permits a wide range of bandwidth-dependent climate record extractions and their subsequent analysis (e.g. as with XWT) and comparison between urban and rural data sources. A method could be developed to determine the degrees of freedom of bandwidth, mother wavelet and time resolution dependent wavelet amplitudes to better test the significance of potential relationships.

#### Acknowledgements

This study was funded by a National Science and Engineering Research Council of Canada Discovery Grant held by Jan

Adamowski. The authors would like to thank P. Larson from the Rideau River Valley Conservation authority for providing streamflow data, and two anonymous reviewers for their suggestions.

#### References

- Abdul Aziz, O.I., Burn, D.H., 2006. Trends and variability in the hydrological regime of the Mackenzie River Basin. *J. Hydrol.* 319 (1–4), 282–294. <http://dx.doi.org/10.1016/j.jhydrol.2005.06.039>.
- Adamowski, J.F., 2008. Development of a short-term river flood forecasting method for snowmelt driven floods based on wavelet and cross-wavelet analysis. *J. Hydrol.* 353 (3–4), 247–266. <http://dx.doi.org/10.1016/j.jhydrol.2008.02.013>.
- Adamowski, K., Prokoph, A., Adamowski, J., 2009. Development of a new method of wavelet aided trend detection and estimation. *Hydrol. Process.* 23 (18), 2686–2696. <http://dx.doi.org/10.1002/hyp.7260>.
- Al-Smadi, A., 2005. Tests for Gaussianity of a stationary time series. *World Acad. Sci. Eng. Technol.* 10, 120–124.
- Anctil, F., Coulibaly, P., 2004. Wavelet analysis of the interannual variability in Southern Quebec streamflow. *J. Clim.* 17 (1), 163–173. [http://dx.doi.org/10.1175/1520-0442\(2004\)017<0163:WAOTIV>2.0.CO](http://dx.doi.org/10.1175/1520-0442(2004)017<0163:WAOTIV>2.0.CO).
- Arnfield, A.J., 2003. Two decades of urban climate research: a review of turbulence, exchanges of energy and water, and the urban heat island. *Int. J. Climatol.* 23, 1–26. <http://dx.doi.org/10.1002/joc.859>.
- Burn, D.H., Fan, L., Bell, G., 2008. Identification and quantification of streamflow trends on the Canadian Prairies. *Hydrol. Sci.* 53 (3), 538–549. <http://dx.doi.org/10.1623/hysj.53.3.538>.
- Coulibaly, P., 2006. Spatial and temporal variability of Canadian seasonal precipitation (1900–2000). *Adv. Water Resour.* 29 (12), 1846–1865. <http://dx.doi.org/10.1016/j.advwatres.2005.12.013>.
- Davis, J.C., 1986. *Statistics and Data Analysis in Geology*. Wiley, New York, 646pp.



- Douglas, E.M., Vogel, R.M., Kroll, C.N., 2000. Trends in floods and low flows in the United States: impact of spatial correlation. *J. Hydrol.* 240 (1), 90–105. [http://dx.doi.org/10.1016/S0022-1694\(00\)00336-X](http://dx.doi.org/10.1016/S0022-1694(00)00336-X).
- Gilbert, R.O., 1987. *Statistical Methods for Environmental Pollution Monitoring*. Van Nostrand Reinhold, New York, 320pp.
- Granato, G.E., 2009. Computer Programs for Obtaining and Analyzing Daily Mean Streamflow Data from the U.S. Geological Survey National Water Information System Web Site: U.S. Geological Survey Open-File Report 2008-1362, 123pp.
- Hinkel, K.M., Nelson, F.E., Klene, A.E., Bell, J.H., 2003. The urban heat island in winter at Barrow, Alaska. *Int. J. Climatol.* 23, 1889–1905. <http://dx.doi.org/10.1002/joc.971>.
- Howard, L., 1833. *Climate of London Deduced from Meteorological Observations*. third ed., vol. 1. Harvey and Darton, London, 348pp.
- Jury, M.R., Enfield, D.B., Mélice, J., 2002. Tropical monsoons around Africa: stability of El Niño–Southern Oscillation associations and links with continental climate. *J. Geophys. Res.* 107, 3151–3167.
- Karaca, M., Tayanç, M., Toros, H., 1995. Effects of urbanization on climate of Istanbul and Ankara. *Atmos. Environ.* 29 (23), 3411–3421. [http://dx.doi.org/10.1016/1352-2310\(95\)00085-D](http://dx.doi.org/10.1016/1352-2310(95)00085-D).
- Karl, T.R., Diaz, H.F., Kukla, G., 1988. Urbanization: its detection and effect in the United States climate record. *J. Clim.* 1 (11), 1099–1123. [http://dx.doi.org/10.1175/1520-0442\(1988\)001<1099:UIDAEI>2.0.CO;2](http://dx.doi.org/10.1175/1520-0442(1988)001<1099:UIDAEI>2.0.CO;2).
- Kendall, M.G., 1975. *Rank Correlation Methods*, forth ed. Charles Griffin, London.
- Kinouchi, T., Yagi, H., Miyamoto, M., 2007. Increase in stream temperature related to anthropogenic heat input from urban wastewater. *J. Hydrol.* 335 (1–2), 78–88. <http://dx.doi.org/10.1016/j.jhydrol.2006.11.002>.
- Krakauer, N.Y., Fung, I., 2008. Is streamflow increasing? Trends in the coterminous United States. *Hydrol. Earth Syst. Sci. Discuss.* 5, 785–810.
- Labat, D., 2008. Wavelet analysis of the annual discharge records of the world's largest rivers. *Adv. Water Resour.* 31 (1), 109–117.
- Lettenmaier, D.P., Wood, E.F., Wallis, J.R., 1994. Hydro-climatological trends in the continental United States, 1948–88. *J. Clim.* 7 (4), 586–607. [http://dx.doi.org/10.1175/1520-0442\(1994\)007<0586:HCTITC>2.0.CO;2](http://dx.doi.org/10.1175/1520-0442(1994)007<0586:HCTITC>2.0.CO;2).
- Li, Q., Zhang, H., Liu, X., Huang, J., 2004. Urban heat island effect on annual mean temperature during the last 50 years in china. *Theor. Appl. Climatol.* 79 (3–4), 165–174. <http://dx.doi.org/10.1007/s00704-004-0065-4>.
- Lin, C.Y., Chen, W.C., Chang, P.L., Sheng, Y.F., 2011. Impact of the urban heat island effect on precipitation over a complex geographic environment in Northern Taiwan. *J. Appl. Meteorol. Climatol.* 50 (2), 339–353. <http://dx.doi.org/10.1175/2010JAMC2504.1>.
- Manley, G., 1958. On the frequency of snowfall in metropolitan England. *Q. J. R. Meteorol. Soc.* 84, 70–72. <http://dx.doi.org/10.1002/qj.49708435910>.
- Mann, S., Haykin, S., 1992. Adaptive “chirplet” transform: an adaptive generalization of the wavelet transform. *Opt. Eng.* 31 (6), 1243–1256.
- Maraun, D., Kurths, J., 2004. Cross wavelet analysis: significance testing and pitfalls. *Nonlin. Process. Geophys.* 11, 505–514.
- Montávez, J.P., Rodríguez, A., Jiménez, J.I., 2000. A study of the heat island of Granada. *Int. J. Climatol.* 20, 899–911. [http://dx.doi.org/10.1002/1097-0088\(20000630\)20:8<899::AID-JOC433>3.0.CO;2-I](http://dx.doi.org/10.1002/1097-0088(20000630)20:8<899::AID-JOC433>3.0.CO;2-I).
- Morlet, J., Arens, G., Fourgeau, I., Giard, D., 1982a. Wave propagation and sampling theory – Part I: complex signal and scattering in multilayered media. *Geophysics* 47 (2), 203–221. <http://dx.doi.org/10.1190/1.1441328>.
- Morlet, J., Arens, G., Fourgeau, I., Giard, D., 1982b. Wave propagation and sampling theory – Part II: sampling theory and complex waves. *Geophysics* 47 (2), 222–236. <http://dx.doi.org/10.1190/1.1441329>.
- Moshin, T., Gough, W.A., 2012. Characterization and estimation of urban heat island at Toronto: impact of the choice of rural sites. *Theoret. Appl. Climatol.* 108 (1–2), 105–117. <http://dx.doi.org/10.1007/s00704-011-0516-7>.
- Nakken, M., 1999. Wavelet analysis of rainfall-runoff variability isolating climatic from anthropogenic patterns. *Environ. Model. Softw.* 14 (4), 283–295. [http://dx.doi.org/10.1016/S1364-8152\(98\)00080-2](http://dx.doi.org/10.1016/S1364-8152(98)00080-2).
- Oke, T.R., 1973. City size and the urban heat island. *Atmos. Environ.* 7 (8), 769–779. [http://dx.doi.org/10.1016/0004-6981\(73\)90140-6](http://dx.doi.org/10.1016/0004-6981(73)90140-6).
- Oke, T.R., Maxwell, G.B., 1975. Urban heat island dynamics in Montreal and Vancouver. *Atmos. Environ.* 9 (2), 191–200. [http://dx.doi.org/10.1016/0004-6981\(75\)90067-0](http://dx.doi.org/10.1016/0004-6981(75)90067-0).
- Prokoph, A., Barthelmes, F., 1996. Detection of nonstationarities in geological time series: wavelet transform of chaotic and cyclic sequences. *Comput. Geosci.* 22 (10), 1097–1108. [http://dx.doi.org/10.1016/S0098-3004\(96\)00054-4](http://dx.doi.org/10.1016/S0098-3004(96)00054-4).
- Prokoph, A., Patterson, R.T., 2004. Application of wavelet and regression analysis in assessing temporal and geographic climate variability: Eastern Ontario, Canada as a case study. *Atmosphere–Ocean* 42 (3), 201–212. <http://dx.doi.org/10.3137/ao.420304>.
- Rioul, O., Vetterli, M., 1991. Wavelets and signal processing. *IEEE Signal Process. Mag.* 8 (4), 14–38. <http://dx.doi.org/10.1109/79.91217>.
- Salmi, T., Määttä, A., Anttila, P., Ruoho-Airola, T., Amnell, T., 2002. Detecting Trends of Annual Values of Atmospheric Pollutants by the Mann-Kendall Test and Sen's Slope Estimates – The Excel Template Application MAKESENS. Publications on Air Quality. No. 31. Finnish Meteorological Institute, Finland, 35pp. <[http://www.ilmanlaatu.fi/ilmansaasteet/julkaisu/pdf/MAKESENS-Manual\\_2002.pdf](http://www.ilmanlaatu.fi/ilmansaasteet/julkaisu/pdf/MAKESENS-Manual_2002.pdf)> (accessed 14.02.13).
- Schaeffli, B., Zehe, E., 2009. Hydrological model performance and parameter estimation in the wavelet-domain. *Hydrol. Earth Syst. Sci.* 13 (10), 1921–1936.
- Shepherd, J.M., Burian, S.J., 2003. Detection of urban-induced rainfall anomalies in a major coastal city. *Earth Interact.* 7, 1–17. [http://dx.doi.org/10.1175/10873562\(2003\)007<0001:DOUIRA>2.0.CO;2](http://dx.doi.org/10.1175/10873562(2003)007<0001:DOUIRA>2.0.CO;2).
- Stewart, I.D., 2000. Influence of meteorological conditions on the intensity and form of the urban heat island effect in Regina. *Can. Geogr.* 44 (3), 271–285. <http://dx.doi.org/10.1111/j.1541-0064.2000.tb00709.x>.
- Torrence, C., Compo, G.P., 1998. A practical guide to wavelet analysis. *Bull. Amer. Meteorol. Soc.* 79 (1), 61–78. [http://dx.doi.org/10.1175/1520-0477\(1998\)079<0061:APGTWA>2.0.CO;2](http://dx.doi.org/10.1175/1520-0477(1998)079<0061:APGTWA>2.0.CO;2).
- Ware, D.M., Thomson, R.E., 2000. Interannual to multidecadal timescale climate variations in the Northeast Pacific. *J. Clim.* 13 (18), 3209–3220. [http://dx.doi.org/10.1175/1520-0442\(2000\)013<3209:ITMTCV>3E2.0.CO;2](http://dx.doi.org/10.1175/1520-0442(2000)013<3209:ITMTCV>3E2.0.CO;2).
- Yague, C., Zurita, E., 1991. Statistical Analysis of the Madrid Urban Heat Island. *Atmos. Environ.* 25B (3), 327–332. [http://dx.doi.org/10.1016/0957-1272\(91\)90004-X](http://dx.doi.org/10.1016/0957-1272(91)90004-X).
- Yalcin, T., Yetemen, O., 2009. Local warming of groundwaters caused by the urban heat island effect in Istanbul, Turkey. *Hydrogeol. J.* 17 (5), 1247–1255. <http://dx.doi.org/10.1007/s10040-009-0474-7>.
- Yulianti, J.S., Burn, D.H., 1998. Investigating links between climatic warming and low streamflow in the prairies region of Canada. *Can. Water Resour. J.* 23 (1), 45–60. <http://dx.doi.org/10.4296/cwrj2301045>.
- Zhang, X., Harvey, K.D., Hogg, W.D., Yuzuk, R., 2001. Trends in Canadian streamflow. *Water Resour. Res.* 37 (4), 987–999. <http://dx.doi.org/10.1029/2000WR900357>.